A Comparison of the Binding of the Ligand Trimethoprim to Bacterial and Vertebrate Dihydrofolate Reductases

ARTICLE *in* ISRAEL JOURNAL OF CHEMISTRY · JANUARY 1986

Impact Factor: 2.22 · DOI: 10.1002/ijch.198600029

A Comparison of the Binding of the Ligand Trimethoprim to Bacterial and Vertebrate Dihydrofolate Reductases

VICTORIA A. ROBERTS,[a] PNINA DAUBER-OSGUTHORPE,[a,c] DAVID J. OSGUTHORPE,[a,c] EUGENE LEVIN[b] AND ARNOLD T. HAGLER[a]*

[a]Agouron Institute, 505 Coast Blvd. So., La Jolla, CA 92037, USA; and
[b]Research Institute for Advanced Computation, Moffett Field, CA 94035, USA;
[c]Present address: School of Chemistry, University of Bath, Bath, BA2 7AY, UK

(*Received 17 April 1986*)

Abstract. In this paper, we report on studies of ligand binding to the enzyme dihydrofolate reductase (DHFR). Energy minimizations of four complexes of DHFR with the inhibitor trimethoprim, an antibiotic, and the cofactor NADPH have been carried out in order to investigate the energetics responsible for the 100,000-fold increase in binding affinity of trimethoprim to *E. coli* DHFR compared with chicken liver DHFR. Several factors suggested to be responsible for the enhanced binding in bacterial DHFR's were investigated in terms of intermolecular and intramolecular energetics. The strain energies of trimethoprim in the four complexes were calculated and found to be about 6 kcal mol^{-1} in all complexes of the two species. In the binary complex of chicken liver DHFR, where the largest variation was observed, 2 kcal mol^{-1} higher than in the other complexes, it was found that this increase was compensated for by the slightly more favorable intermolecular interaction of the trimethoxyphenyl moiety with the protein.

Comparison of the minimized binary and ternary complexes of *E. coli* allowed us to investigate the cooperativity in the binding of trimethoprim and NADPH in the bacterial enzyme in terms of the underlying intermolecular forces. This cooperativity was found to be due to a direct trimethoprim – NADPH interaction in the *E. coli* enzyme rather than enhanced protein–inhibitor interactions induced upon binding of the cofactor. These interactions are not as favorable in the vertebrate enzyme, consistent with the significantly diminished cooperativity observed in this enzyme.

INTRODUCTION

The enzyme dihydrofolate reductase (DHFR) catalyzes the reduction of dihydrofolate to tetrahydrofolate, which is a cofactor involved in the biosynthesis of thymidylate that, in turn, is essential for DNA synthesis.[1-3] Obstruction of the activity of DHFR causes cessation of DNA synthesis and ultimately cell death. Despite the high structural homology of DHFR's across species, several inhibitors have been developed that exhibit high selectivity towards one species of DHFR in the presence of another. In particular, the inhibitor trimethoprim, a clinically used antibiotic, binds 100,000 times more tightly to bacterial DHFR's than to vertebrate DHFR's.[4-7] Part of this enhanced binding to *E. coli* DHFR is due to cooperativity between trimethoprim and the cofactor reduced nicotinamide adenine dinucleotide phosphate (NADPH), a phenomenon observed to a much lesser degree in the vertebrate enzymes. In preliminary studies, we have investigated the energetics and entropics of methotrexate binding to bacterial DHFR.[8] Here we continue the studies of the DHFR system by examining *E. coli* and chicken liver DHFR's by minimization of the potential energy in order to determine the structural and energetic basis of the specificity of trimethoprim binding in this important enzyme.

Numerous high resolution X-ray structures of various DHFR's with several inhibitors have been solved.[9-15] This accurate source of structural information can be used, in addition to supplying initial coordinates, to assess the degree to which the simulation reproduces the details of the observed structure. This, in turn, may be used as an indicator of the reliability of the energetic results and the strategy to be used in interpreting these values.

This paper reviews the simulations of four systems: (1) *E. coli* DGFR with trimethoprim; (2) *E. coli* DGFR with trimethoprim and the cofactor NADPH; (3) chicken liver DHFR with trimethoprim; and (4) chicken liver DHFR with trimethoprim and the cofactor NADPH. Our objectives are to probe the energetic basis of several aspects of the structure and function of this enzyme system. These imply addressing such questions as: What is the basis of selectivity of trimethoprim between the bacterial and vertebrate enzymes? Why does NADPH exhibit cooperativity in the *E. coli* enzyme but not in the chicken liver? What is the strain imposed upon trimethoprim and NADPH upon binding to the enzymes and does this play a part in selectivity? Does the binding of NADPH have long range effects on the enzyme structure? What is the importance of waters in the active site?

These simulations constitute the first step in designing new, more selective DHFR inhibitors and, more generally, in developing methodology based on energetics for investigation of specificity of ligand binding to proteins. The work is being extended to the study of mutations of DHFR and the prediction of the structural and energetic properties of these mutations.

* Author to whom correspondence should be addressed.

COMPUTER SIMULATIONS OF PROTEINS

Both energy minimization techniques and molecular dynamics have been used to investigate protein structure.[16,17] To simulate a complete enzyme complex in water, *ab initio*, would require inclusion of thousands of waters and several counter-ions, as well as all atoms of the proteins and any inhibitor or cofactor of the complex, resulting in extremely large systems. Because of the inordinate computer resources this would require, several approximations have been invoked in previous studies to create complexes small enough to be studied routinely by computer simulations. Most simulations of proteins to date have used a united atom approximation where some or all of the nonpolar hydrogen atoms are incorporated into their carbon atoms. Another approach to reducing system size has been to omit a substantial part of the protein and examine only the active site. These methods have been used, for example, to investigate different substrates binding to α-chymotrypsin[18] and to prealbumin.[19] In addition, cutoff distance is generally applied so that a much smaller number of nonbond interactions need to be calculated.[16,20,21]

A major open question in simulations of protein complexes is how to adequately account for electrostatic energies and forces. Electrostatic forces play a key role in the determination of protein structure and interactions between one group and another in protein complexes. Various dielectric models have been used in an attempt to account for dielectric effects, ranging from a distance-dependent dielectric of R (where R is the distance between the two atoms being analyzed) to constants of 1 to 4. The aqueous environment of the surface increases the apparent dielectric constant that would be used to determine the electrostatic interactions between charged groups on the surface of the protein and charged groups in the interior and problems with these simple models have been pointed out recently.[22] Classical electrostatic theory[23-25] indicates that the effective dielectric constant between two atoms depends both on their separation and on their relative positions in the protein, and the application of such treatments holds promise for future energetic simulations.[22]

Several years ago, we embarked on studies of ligand binding to enzymes using the dihydrofolate reductase system, in which our goals were twofold: first, to calculate the effect of entropy on binding and second, to minimize the number of assumptions in an attempt to provide a basis against which the validity of commonly used approximations might be tested.[8,26] In the simulations reported here, which are a continuation of this work, all hydrogen atoms, polar and nonpolar, are included. We have found that explicit inclusion of all hydrogens in the *E. coli* binary complex, as opposed to the use of "united" atoms, resulted in a significantly better fit of the minimized structure to the experimental structure, especially in the active site region (submitted). No cutoff value has been used and the entire protein, the inhibitor trimethoprim, the cofactor NADPH, and several hundred waters in the active site and around NADPH have been included. Several dielectric models have been assessed in order to get upper and lower bounds on this effect.

METHODS

The potential energy, V, of a system is represented by an analytical function, in this case a valence force field, involving the internal coordinates and the nonbonded interactions within the system (Eq. 1).[27-32]

$$\begin{aligned} V = {} & \sum \{D_b[1 - e^{-\alpha(b-b_0)}]^2 - D_b\} + \tfrac{1}{2}\sum H_\theta(\theta - \theta_0)^2 \\ & + \frac{1}{2}\sum H_\phi(1 + s\cos n\phi) + \tfrac{1}{2}\sum H_\chi \chi^2 \\ & + \sum\sum F_{bb'}(b - b_0)(b' - b_0') \\ & + \sum\sum F_{\theta\theta'}(\theta - \theta_0)(\theta' - \theta_0') \\ & + \sum\sum F_{b\theta}(b - b_0)(\theta - \theta_0) \\ & + \sum F_{\phi\theta\theta'}\cos\phi(\theta - \theta_0)(\theta' - \theta_0') + \sum\sum F_{\chi\chi'}\chi\chi' \\ & + \sum \varepsilon[2(r^*/r)^{12} - 3(r^*/r)^6] + \sum q_i q_j / r. \end{aligned} \tag{1}$$

Basically, the terms in Eq. (1) represent the energies required to deform each internal coordinate from some unperturbed standard value denoted by the subscript 0. There are two types of quantities represented in the equation: constants characteristic of the energy required to deform a given internal coordinate ($D_b \cdots F_{bb}, F_{\theta\theta} \cdots$) or characteristic of the strength of a given interatomic nonbonded interaction (r^* and ε, the size of the atoms and the strength of the van der Waals interaction between them, and q, the partial charges carried by each atom), and the internal coordinates specifying the geometry of the molecule (bond lengths, b; bond angles, θ; dihedral angles, ϕ; out of plane angles, χ; and nonbonded interatomic distances, r). These parameters have been obtained by fitting calculated crystal structures, vibrational frequencies, sublimation energies, and other physical properties of small molecules to their experimentally determined values. The same force field that has been used for small molecules, which includes cross terms, is used here for the entire enzyme complex with no further approximations. As noted above, we have used no cutoff distance, all nonbonded interactions have been calculated, and the effect of different dielectric models has been evaluated.

From the energy surface, we can obtain the forces on the individual atoms by calculating the negative of the first derivatives of the energy with respect to the Cartesian coordinates of the atoms. By solving for the coordinates at which all of the forces are zero, we can obtain the minimum energy conformation for the system. The frequencies and normal modes of the minimum energy conformation can be determined from the matrix of the mass-weighted second derivatives of the energy with respect to the coordinates. The conformational entropy and free energy can then be calculated from the vibrational spectrum in the harmonic approximation through the Einstein relations.[8,17,33]

System Setup

Two sets of refined crystal coordinates were available to us from which we obtained initial atomic positions for these complexes: the refined *E. coli* binary complex of DHFR and trimethoprim (R value of 0.19), and the refined chicken liver ternary complex of DHFR, trimethoprim, and NADPH (R value of 0.22).[9] No crystal of *E. coli* DHFR with NADPH has been obtained and thus no structure exists. Therefore, the *E. coli*

ternary complex was built from the coordinates of the binary complex with NADPH where the coordinates of NADPH were obtained from the ternary complex of *L. casei* DHFR with methotrexate and NADPH by superposition.[9] To create initial coordinates for the chicken liver binary complex, NADPH was removed from the ternary complex and replaced by water molecules.

To complete the setup of the initial coordinates, waters that may play an important role in the structure of these complexes were added. Crystallographically determined waters within 7 Å of trimethoprim and NADPH were included. Crystal waters that appear to play a structural role in the protein structure, i.e. those that form a bridge through hydrogen bonds from one segment of the protein to another, were also included. Waters were generated to fill the area within 7 Å of NADPH and trimethoprim, and within 3 Å of all charged residues. Thus, we have built these complexes so that the principal area of interest, the active site, is completely solvated out to 7 Å.

Minimization

The protein complexes were gradually relaxed to relieve unfavorable initial interactions. First, the energy was minimized allowing only the water molecules to relax with the oxygen atoms lightly constrained in order to adjust the positions of the water hydrogens and relieve clashes between some of the poorly determined crystal waters and the protein. In the next stage, all atoms were allowed to relax with the heavy atoms lightly constrained to relieve unfavorable interactions between poorly defined atoms or between the hydrogens added to the protein and trimethoprim. Finally, the energy of the system was minimized with respect to all $3N$ Cartesian coordinates of the system until the average first derivative was less than 0.001 kcal mol^{-1} Å^{-1} (corresponding to a maximum first derivative of less than 0.025 kcal mol^{-1} Å^{-1} and a change in energy of less than 0.00005 kcal mol^{-1} in the last step). These unconstrained minimizations required between 10,000 and 16,000 iterations, which took between 15 to 20 hours of CPU time on the Cyber 205 supercomputer.

A dielectric constant of one was used for these minimizations and the final minimized structures were evaluated using this dielectric. We have also examined the effects of larger dielectric constants or a distance-dependent dielectric on the energetics of the final minimized structures.

COMPARISON OF SIMULATED DHFR COMPLEXES WITH EXPERIMENTAL STRUCTURES

A common measure of the fit of two protein structures that can be employed to obtain a quantitative comparison is the root mean square (RMS) deviation of corresponding atoms in the two superimposed structures. Although this is useful as an overall indicator, a detailed assessment of structural similarity requires detailed local information, as discussed below. Because loops connecting secondary structures tend to be more disordered than the secondary structures themselves, we have superimposed the calculated and observed structures using a least squares fit of the heavy atoms of their secondary structures, i.e. the α helices and β strands. This avoids artifacts in the superposition arising from bias due to poorly defined regions or loops at the surface. Given this superposition, the root mean square (RMS) deviation can then be calculated for the entire protein, to give a general idea of the degree of fit, or for local regions such as the active site, to indicate the distribution of movement throughout the protein complex.

Internal regions of the protein, such as the active site, are expected to fit the experimental structure more accurately than areas on the surface of the protein, which are less well-defined in the experimental structure and may be involved in intermolecular, lattice interactions with neighboring protein and solvent molecules. Most of the residues with large RMS values (greater than 1.5 Å) lie in external loops (between βC and βD, between βF and βG, or, in chicken liver in the large external "β-bulge" in βG) that show substantial disorder in the experimental structure (Fig. 1).

One example of the effect of the crystal environment on the structural features of the protein may be seen from the comparison of the positions of Glu^{161} on the βG strand in the observed and minimized chicken liver DHFR complexes. This is the residue with the largest RMS deviation from the experimental structure in both the ternary and binary minimized complexes. In the experimental structure, this residue forms an intermolecular hydrogen bond with Arg^{132} of an adjacent protein molecule. In the minimized structures, Glu^{161} has undergone substantial movement (RMS deviation of about 6 Å) to form an intramolecular hydrogen bond with Arg^{132}. Thus, the lack of specific intermolecular interactions is responsible for a large RMS deviation. (This may also be an example of an intramolecular hydrogen bond that is formed in solution but not in the crystalline state.)

The well-defined areas of the protein, such as the active site and the C_α carbons of the α helices and β strands, on the other hand, show RMS deviations substantially lower than that of the overall protein (Table I). The pyrimidine ring of trimethoprim, deep in the active site cleft, has an RMS deviation from the experimentally observed structure less than that of the trimethoxyphenyl moiety, which extends out towards the surface of the protein. Similarly, in the chicken liver ternary complex, the nicotinamide ring, which extends into the active site, has a much smaller RMS deviation (0.34 Å), than the NADPH molecule as a whole, which generally lies on the surface of the protein. (In the *E. coli* ternary complex, the overall RMS deviation of NADPH is larger, probably because it was built into the crystal structure of the observed *E. coli* binary complex by structural homology.) Thus, the crucial area for this study, the active site, shows good agreement with the experimental structure.

Comparison of the Active Site Region

The ligand and its nearest neighbors are depicted schematically in Figure 2 for the *E. coli* and Figure 3 for the chicken liver experimental and minimized complexes. The pyrimidine moiety of trimethoprim is involved in an extensive hydrogen bond network to the protein both directly and through water molecules. The major difference between the hydrogen bonding pattern in the two species lies in the hydrogen bond between N4 of the pyrimidine ring and the carbonyl oxygen of Ile^{94} (2.9 Å in the *E. coli* complex), and the lack of this hydrogen bond with the corresponding carbonyl oxygen of Val^{115} (homologous to Ile^{94}) in the chicken liver complex (N4–O distance of 4.1 Å).[9]

In the *E. coli* complexes, the hydrogen bonding pattern is maintained in the minimized structures. In the *E. coli* binary complex (Figs. 2A and 2B), a water molecule

(H_2O 39, a water defined in the observed structure) has moved to form a hydrogen bond with N4 of the pyrimidine ring, while maintaining a hydrogen bond with the carbonyl oxygen of Ile[94]. In the ternary complex (Fig. 2C), this water is displaced by the nicotinamide ring of NADPH (not shown). In the minimized binary complex of the chicken liver DHFR (Fig. 3B), the distance between the carbonyl oxygen of Val[115] and N4 of the pyrimidine ring has lengthened slightly (from 4.1 A to 4.4 Å), and a water molecule (H_2O 326, a water generated to replace NADPH in the initial binary structure, see Fig. 3A) forms a hydrogen bond to each of these atoms. The situation, except for the longer N4–carbonyl oxygen distance, is similar to that of the *E. coli* binary complex with a water mediating the interactions between these two groups. In the minimized ternary chicken liver complex (Fig. 3C), however, the distance between N4 and the carbonyl oxygen of Val[115] has shortened to 3.0 Å, forming a hydrogen bond. The lack of this hydrogen bond in the observed chicken liver complex has been suggested to be the major factor responsible for the poorer binding of trimethoprim in vertebrate as com-

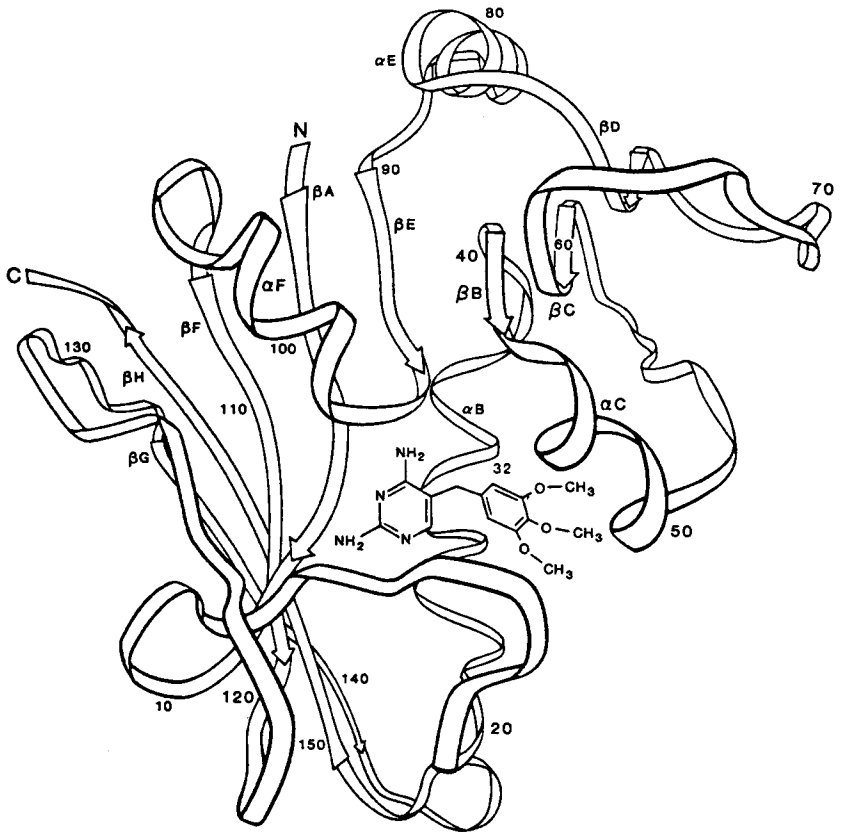

Fig. 1. Schematic representation of *E. coli* DHFR showing relative positions of α helices, β strands, and the loops connecting them. The bound inhibitor trimethoprim in the active site is also indicated. This figure is adapted from Ref. 10.

Table I. RMS Deviations for Heavy Atoms and C_α Atoms Between the Minimized and the Observed Structures[a] (in Å)

Region	*E. coli* Binary	*E. coli* Ternary	Chicken Liver Binary	Chicken Liver Ternary
All Heavy Atoms[b]	1.23 (1.07)	0.94 (0.72)	1.47 (1.10)	1.49 (1.10)
Trimethoprim	0.81	0.69	0.42	0.68
Pyrimidine ring	0.42	0.55	0.24	0.65
Trimethoxyphenyl ring	0.97	0.74	0.50	0.70
NADPH	—	0.95	—	0.67
Active site[c]	0.58 (0.54)	0.50 (0.41)	0.60 (0.51)	0.72 (0.57)
α helices	1.10 (0.72)	0.81 (0.47)	0.99 (0.64)	1.02 (0.76)
β strands	0.82 (0.66)	0.68 (0.47)	1.34 (1.00)	1.34 (0.89)

a. Numbers in parentheses are the RMS deviations of C_α atoms.
b. Deviations of water molecules are not included.
c. Residues with any atom within 4 Å of trimethoprim.

pared with bacterial DHFR's.[6,9] As discussed below, a comparison of the initial complex and the ternary minimized complex allows us to approximate the cost of the loss of this hydrogen bond. From both these calculations and other experimental data,[34] it would appear that, although significant, the strain induced in this hydrogen bond is not, in and of itself, sufficient to account for the full decrease in binding affinity.

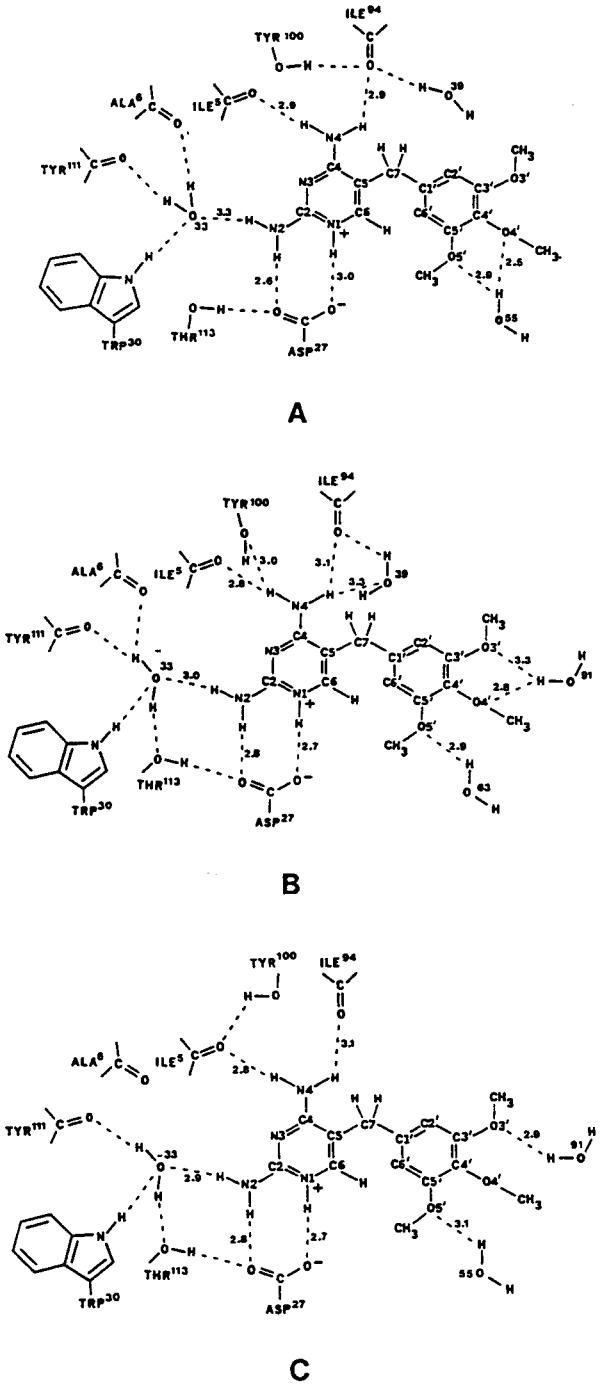

Fig. 2. Schematic diagrams of the active site of the *E. coli* complexes in A) the observed binary structure, B) the minimized binary structure, and C) the minimized ternary structure (NADPH is not shown). Hydrogen bonds are indicated by dashed lines, the numbers on these bonds refer to the distance (in Å) between the heavy atoms (N and O). The orientation of these diagrams is close to that of the stereo plot in Fig. 5. Residues Trp^{30} and Ala^{8} are reoriented somewhat for clarity.

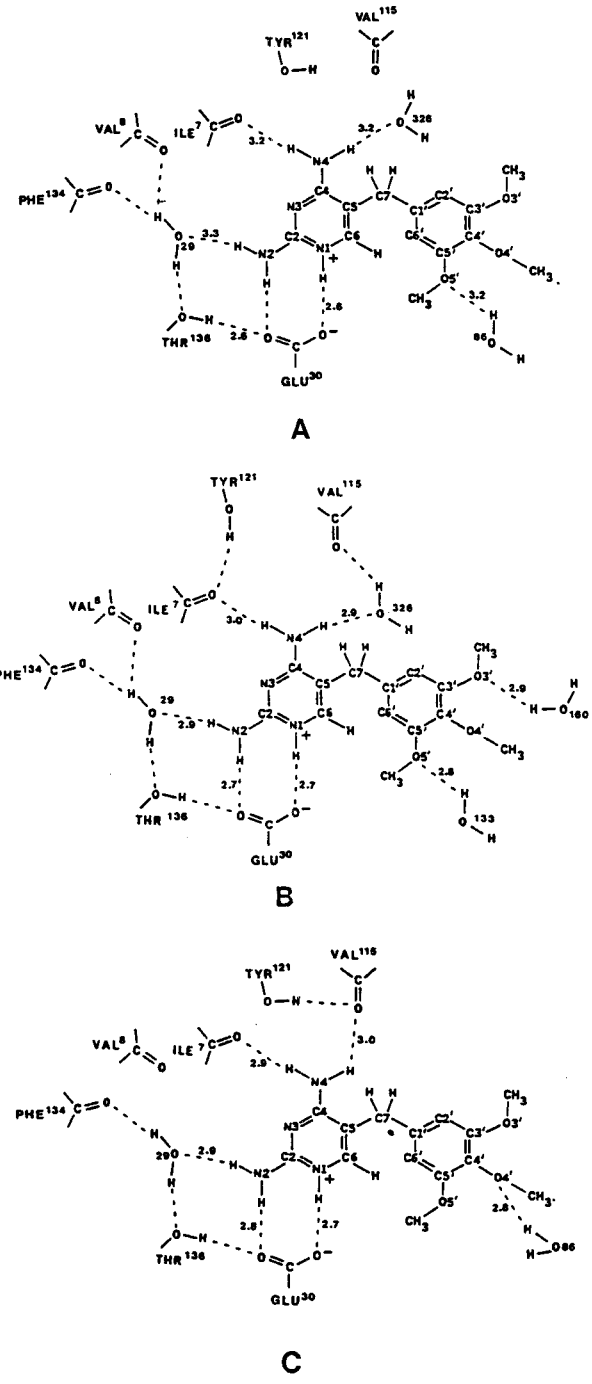

Fig. 3. Schematic diagrams of the active site of the chicken liver complexes in A) the initial binary structure (with NADPH in the observed structure replaced by waters), B) the minimized binary structure, and C) the minimized ternary structure (NADPH is not shown). Hydrogen bonds are indicated by dashed lines, the numbers on these bonds refer to the distance (in Å) between the heavy atoms (N and O). The orientation of these diagrams is close to that of the stereo plot in Fig. 6. Residue Val^{8} is reoriented somewhat for clarity.

In both the experimental chicken liver and *E. coli* complexes, the trimethoxyphenyl ring of trimethoprim interacts with the protein through nonspecific van der Waals interactions. Although there is some movement of this ring relative to the protein, especially in the *E. coli* binary complex, for the most part the protein adjusts its position to maintain these nonspecific interactions. Thus, although the RMS deviations of the trimethoxyphenyl ring of trimethoprim and the neighboring residues of DHFR (predominantly the αC helix) indicate that there are large movements and structural changes in this area of up to an angstrom, the individual interactions appear to be maintained. The RMS deviations here seem indicative of a shallow energy surface where nonspecific van der Waals interactions are retained through an overall correlated shift of both the ligand and protein rather than a disruption of structure.

Comparison of Experimental and Calculated Structures of Trimethoprim

Overall, the general structural features of trimethoprim in the four complexes are maintained in the minimized structures. Trimethoprim has only two major degrees of conformational freedom, involving rotations about the central methylene group (C7), torsion angles τ_1 and τ_2 (see Fig. 4). In the *E. coli* complex, the two aromatic rings are approximately perpendicular to each other as indicated in Fig. 4A and by a τ_1 of 180° and τ_2 of 75°. On the other hand, in the chicken liver complex the two aromatic rings face each other with a τ_1 of $-84°$ and τ_2 of 110° (Fig. 4B). Other bonds with freedom of rotation are the three methoxy groups. Crystal structures of trimethoprim and its derivatives[35,36] and the structure of trimethoxybenzene in solution[37] indicate that the two *meta* methoxy groups prefer to lie close to the plane of the aromatic ring pointing away from the *para* group, while the *para* group prefers to lie out of the plane of the aromatic ring.

The conformation about the methylene group is retained in the minimized structures (Table II). In the minimized *E. coli* binary and ternary complexes, the trimethoprim molecule retains the approximately perpendicular arrangement of the aromatic rings observed in this structure. The appoximately parallel arrangement of rings is maintained in the chicken liver minimized complexes. The methoxy groups rotate substantially about the C–O(CH_3) bonds especially in the chicken liver ternary structure, and, as a result, contribute to the strain energy of the trimethoprim in this complex, as discussed below. In addition to the minimizations of the enzyme complexes, we have taken trimethoprim in the conformation of the initial *E. coli* complex and minimized it as an isolated molecule in order to investigate the strain induced on binding (or crystallization). The arrangement of the methoxy groups in this minimized, isolated structure is similar to that of the crystal structures and that in solution (Table II).

ENERGETIC ANALYSIS OF LIGAND BINDING

The ligand trimethoprim is known to inhibit *E. coli* DHFR some 10^5 times more strongly than chicken liver DHFR in the presence of NADPH.[4-7] This selectivity is partly dependent on enhanced cooperativity by NADPH in the *E. coli* enzyme, in contrast to a much less marked cooperativity exhibited by vertebrate enzymes. Specifically, Baccanari *et al.* have shown that the *E. coli* DHFR dissociation constant for trimethoprim is decreased 40-fold in the presence of NADPH, whereas for rodent

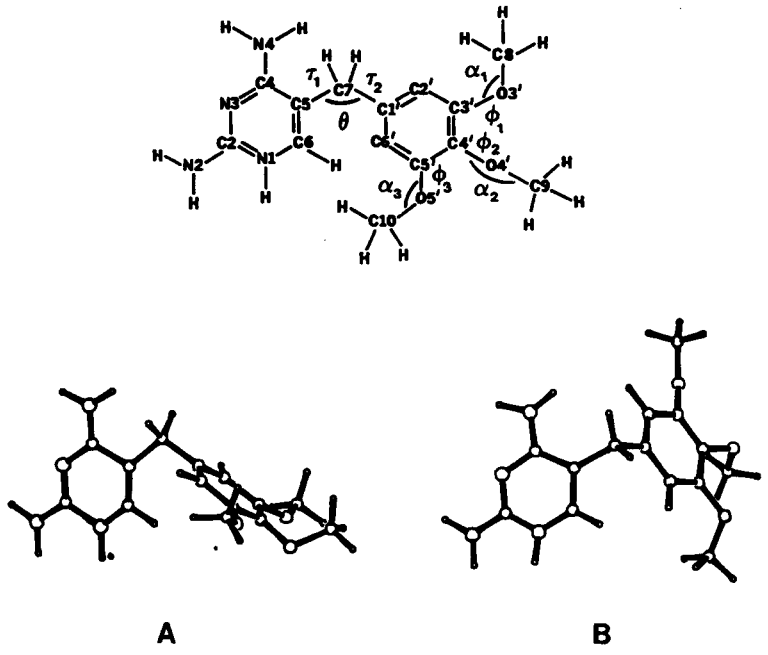

Fig. 4. Nomenclature used in this paper for the molecule trimethoprim showing torsion angles τ_1 (C4–C5–C7–C1′) and τ_2 (C5–C7–C1′–C2′) about the central methylene carbon, C7, and the methoxy group torsion angles ϕ_1 (C2′–C3′–O3′–C8), ϕ_2 (C3′–C4′–O4′–C9), and ϕ_3 (C4′–C5′–O5′–C10). Also shown are the valence angles θ (C5–C7–C1′), α_1 –C3′–O3′–C8), α_2 (C4′–04′–C9), and α_3 (C5′–O5′–C10). The conformation of trimethoprim in the *E. coli* complex is shown in A, with the two aromatic rings approximately perpendicular to each other. The conformation of trimethoprim in the chicken liver complex is shown in B with the two rings facing each other.

lymphoma DHFR the corresponding decrease is only a factor of 2.8.[38] To this point, the mechanism has not been resolved and no examination of the underlying energetics has been presented.

Several explanations for the source of enhanced binding of trimethoprim in bacterial DHFR's have been proposed. The difference in binding has been attributed to an increase in strain energy of trimethoprim induced on binding in mammalian DHFR's,[6] to different interactions in the different binding sites occupied by the trimethoxyphenyl group of trimethoprim in bacterial and mammalian DHFR's,[39] or to a change in hydrogen bonding of the protein to the pyrimidine ring of trimethoprim.[6,9] These different effects are examined below in terms of intermolecular and intramolecular interactions and energetics.

Strain Energy Induced in the Ligand on Binding

It is of interest to assess the strain induced in the ligand on binding to the enzyme.[40] At the current state of protein refinement, one cannot achieve this simply by examination of crystal coordinates since even minimal experimental errors in atomic positions (0.2 Å)[9] lead to large strain energies. This can be seen, for example, by considering a typical bond that has a force constant of about 640 kcal mol^{-1} Å^{-2}. An error of 0.2 Å in bond length gives a strain per bond of 13 kcal mol^{-1}. For a valence angle with a typical force constant of about 100 kcal mol^{-1} radian^{-2}, the strain per angle, if one atom has an error of 0.2 Å, can be as much as 1 kcal mol^{-1}. Specific examples of such distortions can be seen in the observed structure of the *E. coli* binary complex (see Table II) in angles ϕ_1 (134°) and ϕ_3 (142°), which differ substantially from their equilibrium value of about 110°, and contribute 9 and 16 kcal mol^{-1}, respectively, to the valence angle strain energy. These strains due to uncertainties in crystallographic coordinates are reflected in the total components of strain energy given for the initial structures in Table III.

We can calculate, however, the contribution of strain

Table II. Comparison of Valence and Torsion Angles of Trimethoprim in DHFR Complexes

Torsion Angle	Isolated Minimized	*E. coli* Binary Initial	*E. coli* Binary Minimized	*E. coli* Ternary Minimized	Chicken Liver Ternary Initial	Chicken Liver Binary Minimized	Chicken Liver Ternary Minimized
τ_1 (C4–C5–C7–C1′)	−85	180	−155	−163	−84	−88	−95
τ_2 (C5–C7–C1′–C2′)	86	75	63	79	110	112	101
θ (C5–C7–C1′)	112	108	119	118	110	114	114
ϕ_1 (C2′–C3′–O3′–C8)	3	16	5	−2	−21	−35	47
ϕ_2 (C3′–C4′–O4′–C9)	94	65	84	127	−139	−105	−108
ϕ_3 (C4′–C5′–O5′–C10)	174	159	180	161	169	−174	−129
α_1 (C3′–O3′–C8)	126	134	124	124	119	123	121
α_2 (C4′–O4′–C9)	117	111	118	120	123	119	119
α_3 (C5′–O5′–C10)	125	142	124	124	122	124	121

Table III. Energetics and Entropics of the Ligand, Trimethoprim, Bound to the Bacterial and Vertebrate Enzymes and in the Free State (Energies are in kcal mol^{-1})

Energy Component		Bound to DHFR						Isolated
		E. coli Observed	*E. coli* Binary	*E. coli* Ternary	Chicken Observed	Chicken Binary	Chicken Ternary	
Valence	E_b	46.1	27.8	27.3	33.7	26.8	27.0	27.9
	E_θ	49.3	16.7	15.7	25.6	15.1	12.8	16.6
	E_ϕ	7.9	8.1	7.2	4.5	13.0	16.7	7.2
	E_χ	0.0	0.0	0.0	0.0	0.0	0.0	0.0
	$E_{x.t.}$	1.8	2.3	2.3	1.1	2.0	1.8	1.9
	Total Valence	105.2	54.9	52.5	64.9	56.9	58.3	53.6
Intra-molecular	E_{vdw}	93.3	79.8	83.9	120.6	78.4	76.6	76.2
	E_{cou}	−90.8	−92.0	−92.6	−83.6	−90.3	−91.3	−92.3
	Total Nonbond	2.6	−12.2	−8.7	36.9	−11.9	−14.7	−16.1
Total		107.8	42.7	43.8	101.8	45.2	43.6	37.5
Vibrational	Enthalpy	—	218.7	219.2	—	219.1	218.7	213.4
	$T*$Entropy	—	24.2	24.3	—	23.3	24.3	24.2[a]
	Free Energy	—	194.4	194.9	—	195.8	194.5	

[a] There are $3N$-6 degrees of vibrational freedom; the entropies correspond to only $3N$-6 degrees of freedom for the isolated ligand and $3N$ degrees of freedom for the bound ligand. The remaining 6 degrees of freedom in the isolated ligand, of course, correspond to the translation and rotation. Thus, the entropies given here reflect the large loss of entropy on binding corresponding to the translational and rotational entropy. The lowest six vibrational frequencies of the bound ligand contribute about 8 of the 24 kcal per mole of the entropic contribution of the vibrational free energy given in the table.

energy to the binding of trimethoprim by comparing the intramolecular energy of trimethoprim in the bound state in the minimized complexes to the minimum energy of the isolated molecule. Furthermore, by partitioning the energy into its various valence components, we can determine the source of increased strain.[41] The total intramolecular energy (valence and nonbond) of trimethoprim in the isolated molecule is 37.5 kcal mol^{-1}, while the corresponding energies of trimethoprim in the minimized structures range from 42.7 kcal mol^{-1} in the *E. coli* binary complex to 45.2 kcal mol^{-1} in the chicken liver binary complex (Table III). Thus, the strain energy induced in the inhibitor by the enzyme varies from 5.2 to 7.7 kcal mol^{-1}.

Despite the similarity of total strain energy for trimethoprim, the distribution of the strain differs dramatically in the different complexes. The trimethoprim molecule in the chicken liver complexes shows considerably more torsion angle strain than it does in the *E. coli* complexes or in the isolated molecule; this increase is partially compensated for by a decrease in the valence angle strain energies. The increase in torsion angle strain is predominantly due to the methoxy groups on the phenyl ring. In the *E. coli* enzyme, the trimethoxyphenyl moiety extends out into the water-filled cavity leading to the protein surface; it is mainly constrained by the surrounding mobile waters. In the chicken liver enzyme, this group lies in a pocket surrounded by the protein that appears to apply stronger constraints to the methoxy positions, especially to the torsion ϕ_1 in the binary complex and ϕ_1 and ϕ_3 in the ternary complex (Table II). In the minimization, the *meta* methoxy groups of the trimethoprim in the chicken liver complexes are forced out of the plane of the aromatic ring, causing an increase in torsion angle energy (E_ϕ) *relative to the E. coli* complexes. At the same time, the valence angles about the methoxy group oxygens relax slightly from about 125° when the methyl group lies in the plane of the phenyl ring, to an angle closer to 121° (α_1 and α_3 in Table II) because the steric hindrance with the *ortho* hydrogens on the phenyl ring is reduced, resulting in a decrease of the valence angle energy (E_θ) compared with the *E. coli* complexes.

Although the distribution of strain energy of trimethoprim is different in the two species of DHFR, the total strain is similar for all complexes. A comparison of the total strain energy indicates that the difference in binding in the two binary complexes may be due in part to additional strain energy of trimethoprim in the chicken liver complex. On the other hand, the trimethoprim molecule has very similar strain energies in the two ternary complexes, and thus this does not appear be a dominant factor in the difference in binding.

Entropy of the Bound Ligand

An assumption often made in theoretical calculations of the free energy of binding is that the entropic contributions to binding are approximately equal for the binding of similar inhibitors to similar enzymes. Studies on small peptides have indicated that vibrational entropies can be of crucial importance in conformational equilibria.[32] The contribution of the entropy to the energy of binding may be of similar importance. On the other hand, the binding of either the inhibitor methotrexate or folate to chicken liver DHFR has been shown to be principally an enthalpy-driven process.[42] The difference between the entropy of binding in different enzymes can be determined by examination of the same inhibitor, trimethoprim, in the four complexes (Table III). The change in vibrational entropy due to restriction in ligand motion by the protein is similar in all four complexes. Thus, difference in entropy of binding also does not appear to be a major contributing factor to the enhanced binding of trimethoprim to *E. coli* DHFR.

Binding of the Trimethoxyphenyl Group of Trimethoprim

The pyrimidine ring binds in a similar fashion to the protein of both species. The trimethoxyphenyl group, however, lies in different environments in the two complexes as indicated by the different conformations about the methylene group as discussed above. In the *E. coli* complex, this group lies in the cavity extending out of the protein and points towards the putative binding site of nicotinamide ring of NADPH. In the chicken liver complex, this group fits into a side channel and points away from the nicotinamide ring. It has been suggested that the potential for favorable van der Waals contacts of the trimethoxyphenyl group with the binding cleft of chicken liver DHFR is comparable to that of the binding cleft of *E. coli* DHFR because several potent inhibitors of chicken liver DHFR also bind in the same cleft.[6] We have examined the energetics of the trimethoxyphenyl group in both enzymes to investigate quantitatively the difference in energetics of binding in the two sites.

Table IV gives the interactions of the protein, waters, and NADPH for each minimized complex with the trimethoxyphenyl group. There is almost a 10 kcal mol^{-1} difference in the total van der Waals interactions between trimethoprim and the remaining molecules in the *E. coli* binary and chicken liver ternary complexes (-26.3 to 36.2 kcal mol^{-1}). When both van der Waals and coulombic interactions are taken into account, however, the difference in the interactions with the trimethoxyphenyl group in both ternary complexes is only 0.1 kcal mol^{-1} (-45.9 versus -46.0 kcal mol^{-1}). The trimethoxyphenyl ring has the most favorable environment in the chicken liver binary complex, about 3 kcal mol^{-1} more favorable than in the *E. coli* binary complex. Thus, it appears that, if anything, the binding of the trimethoxyphenyl ring may be slightly more favorable in the chicken liver enzyme, and this factor is not responsible for the enhanced trimethoprim binding in *E. coli* DHFR. One important factor that this discussion does not take into account is the amount of strain imposed upon the protein due to binding of the trimethoxyphenyl group in the two enzymes. Determination of this effect requires the further simulation of the two enzymes in the corresponding aqueous environment without the inhibitor.

The determination of the intermolecular interactions of the trimethoxyphenyl group (Table IV) involves calculation of the electrostatics of this group with the charged protein and NADPH. As discussed above, this is one of the least well characterized intermolecular interactions. We can, in this instance, determine upper and lower bounds for this effect and show that the relative favorability is insensitive to the magnitude of the dielectric although, of course, the absolute value of the difference in binding energy to the two enzymes is affected significantly. If a distance-dependent dielectric is used, the total intermolecular interactions of the trimethoxyphenyl group with all other molecules in the complex become -40.4, -41.7, -43.5, and -42.9 for the *E. coli* binary complex, the *E. coli* ternary complex, the chicken liver

Table IV. Intermolecular Interactions of the Trimethoxyphenyl Group of Trimethoprim With Other Molecules in the Complex[a]

	Energy	*E. coli* Binary	*E. coli* Ternary	Chicken Liver Binary	Chicken Liver Ternary
Protein	Van der Waals	−17.7	−18.1	−25.3	−26.5
	Coulomb	0.5	−0.9	−2.6	−3.1
	Total	−17.2	−19.0	−27.9	−29.6
Waters	Van der Waals	−8.6	−7.8	−8.0	−7.5
	Coulomb	−18.4	−10.3	−11.4	−5.4
	Total	−27.0	−18.1	−19.4	−12.9
NADPH	Van der Waals	—	−4.4	—	−2.2
	Coulomb	—	−4.4	—	−1.3
	Total	—	−8.8	—	−3.5
Total	Van der Waals	−26.3	−30.3	−33.3	−36.2
	Coulomb	−17.9	−15.6	−14.0	−9.8
	Total	−44.2	−45.9	−47.3	−46.0

a. Energies are in kcal mol^{-1}.

binary complex, and the chicken liver ternary complex, respectively. Although the absolute numbers are somewhat lower than those calculated using a dielectric of 1, the chicken liver binary complex still retains about a 3 kcal mol^{-1} more favorable interaction than the *E. coli* binary complex (−43.5 versus −40.4 kcal mol^{-1}) with the interactions in the ternary complexes lying between the two. Thus, in this case, a distance-dependent dielectric gives results very similar to those with a dielectric of 1.

If we go to the other extreme and consider the effect of a dielectric of 80 (or even infinity), the electrostatic energies vary from 0.1 to 0.2 kcal mol^{-1} and the results obtained depend solely on the van der Waals interactions given in Table IV. Therefore, this interaction is calculated to be even more favorable in the chicken liver complexes than when calculated using a dielectric constant of 1 or a distance-dependent dielectric. Thus, determination of the intermolecular interactions of the trimethoxyphenyl group by any of these treatments of dielectric leads to the same conclusion: the intermolecular interactions of the trimethoxyphenyl group of trimethoprim are favored in the chicken liver complexes and this factor is not responsible for the enhanced binding of trimethoprim in *E. coli* DHFR compared with vertebrate DHFR's.

Difference of Hydrogen Bonding of the Pyrimidine Ring of Trimethoprim

Crystal structures have indicated there is a loss of one hydrogen bond between N4 of the pyrimidine ring and the protein on going from *E. coli* DHFR to chicken liver DHFR (Ile^{94} to Val^{115}).[9] It has been suggested that this is the major factor responsible for the greater potency of trimethoprim in bacterial DHFR's.[6] As mentioned above, the minimized chicken liver binary complex retains the separation between N4 of the pyrimidine ring and the carbonyl oxygen of Val^{115} that exists in the crystal structure of the chicken liver ternary DHFR complex. In the minimized ternary complex, this distance is decreased to 3.0 Å, thus forming the hydrogen bond. By looking at the interaction energies between Val^{115} and the pyrimidine ring, the energetic difference between these two groups in the binary complex (with a similar N–O distance, 4.4 Å, to that in the observed complex, 4.1 Å) and in the minimized ternary chicken liver complex (with a similar N–O distance, 3.0 Å, to that in the observed *E. coli* complex, 2.9 Å) can be determined.

An examination of the energetics between the carbonyl group of Val^{115} and the 4-amino NH_2 moiety of the pyrimidine ring reveals that the loss of this interaction costs 2.3 kcal mol^{-1}. The energy of interaction in the minimized binary complex is −1.4 kcal mol^{-1}. On the other hand, in the minimized chicken liver ternary complex, where a hydrogen bond has formed between the two groups, the interaction is −3.7 kcal mol^{-1}. In the absence of NADPH, trimethoprim binds about 5000 times more strongly to *E. coli* DHFR than chicken liver DHFR.[7] This corresponds to a difference of about 5 kcal mol^{-1} of binding free energy. Thus, although the loss of the hydrogen bond may account for as much as one half of the loss of binding energy, it does not appear that the difference in this interaction alone can be responsible for the total decrease in binding in vertebrate DHFR's.

It is important, however, to realize that the difference in binding of trimethoprim (and ligands in general) is indubitably due to a large number of effects. We can see an example of this phenomenon by examination of differences of intermolecular interactions of trimethoprim with individual homologous residues in complexes of different species, an example of which is seen in Table V. In the two binary complexes, for example, the more favorable interaction between trimethoprim and Ile^{94} (−6.4 kcal mol^{-1}) and Tyr^{100} (−1.9 kcal mol^{-1}) in the *E. coli* complex compared with Val^{115} (−4.2 kcal mol^{-1}) and Tyr^{121} (0.9 kcal mol^{-1}) in the chicken liver enzyme is offset by less favorable interactions with Phe^{31} (−6.6 kcal mol^{-1}) and Thr^{113} (2.2 kcal mol^{-1}) in *E. coli* compared with Phe^{34} (−10.8 kcal mol^{-1}) and Thr^{136} (1.4 kcal mol^{-1}) in chicken liver. Thus, although the crystallographic data suggests that the lack of the hydrogen bond between trimethoprim and Val^{115} may be responsible for the loss of affinity for trimethoprim in the chicken liver enzyme, there may be compensation elsewhere in protein–ligand interactions or in interactions of the solvent with the inhibitor.

Another example of compensating effects is seen in the example above in which the strain energy of trimethoprim is about 2 kcal mol^{-1} greater in the minimized chicken liver binary complex than in the other three complexes. On the other hand, the intermolecular in-

Table V. Difference of Interactions of Trimethoprim with Selected Active Site Residues Between Chicken Liver and *E. coli* Binary Complexes[a]

E. coli Residue	Chicken Liver Residue	ΔE[b]
Ile^{5}	Ile^{7}	1.4
Ala^{6}	Val^{8}	−0.7
Ala^{7}	Ala^{9}	−1.4
Trp^{30}	Tyr^{33}	0.7
Phe^{31}	Phe^{34}	−4.2
Ile^{94}	Val^{115}	2.2
Tyr^{100}	Tyr^{121}	2.8
Thr^{113}	Thr^{136}	−0.8

a. The difference in energy is the energy of interaction of chicken liver minus that of *E. coli* so that a more favorable chicken liver interaction is indicated by a negative ΔE.
b. Energies in kcal mol^{-1}.

teractions of the trimethoxyphenyl ring are about 2 kcal mol^{-1} more favorable in this complex than in the *E. coli* complexes. Thus, the greater intramolecular strain of trimethoprim in this complex appears to be compensated for by the more favorable intermolecular interactions.

Effect of NADPH on Protein–Ligand Interaction Energy

The cooperativity of NADPH in *E. coli* DHFR has been demonstrated experimentally to be another factor responsible for the enhanced binding of trimethoprim to bacterial DHFR's.[7,38] We have examined these DHFR complexes both with and without NADPH to determine the energetic basis underlying this cooperativity. In principle, the NADPH could induce a conformational change of the protein making it more conducive to the binding of trimethoprim. In fact, and perhaps more to be expected, the opposite occurs. The calculated intermolecular energy between trimethoprim and the protein in the *E. coli* complex was found to be −214.4 kcal mol^{-1} while this energy is −188.7 kcal mol^{-1} in the *E. coli* ternary complex. The major difference in binding energy arises because His^{45} becomes protonated on binding of NADPH, (as evidenced by proton magnetic resonance studies).[43] The interaction of this protonated histidine with the positively charged trimethoprim accounts for 20.9 kcal mol^{-1} of the 25.7 kcal mol^{-1} difference in the interaction energy. The constraints induced by the binding of NADPH also reduce the ability of the protein to accommodate trimethoprim and this is reflected in the additional 4.8 kcal mol^{-1}.

Again, we can obtain bounds on this electrostatic interaction. Different treatments of the dielectric decrease the difference in protein–trimethoprim interactions between the binary and ternary *E. coli* complexes, but this interaction continues to be more favorable in the binary complex. For example, with a distance-dependent dielectric, the protein–ligand interaction is −85.3 kcal mol^{-1} in the binary *E. coli* complex and −83.1 kcal mol^{-1} in the ternary complex. Therefore, this interaction is calculated to be 2.2 kcal mol^{-1} more favorable in the binary complex. Thus the energetic results indicate that binding of NADPH does not predispose the enzyme to interact more favorably with trimethoprim, regardless of treatment of dielectric, and this does not appear to contribute to the observed cooperativity in *E. coli* DHFR.

Enhanced Cooperativity of NADPH in the E. coli Ternary Complex, Interactions Between Trimethoprim and NADPH

Comparison of the interactions of NADPH with trimethoprim in the *E. coli* ternary complex as built by structural homology (see above) and the chicken liver ternary complex gives us a clue as to the source of the enhanced cooperativity of NADPH in the bacterial enzyme. The energy of this interaction in the minimized structures is 6.6 kcal mol^{-1} more favorable in the *E. coli* complex. We have partitioned these interaction energies into the contributions from the various functional groups in order to determine the specific interactions responsible for this difference (Table VI). The pyrimidine group binds similarly in the two enzymes. Therefore, the energetic interaction of the pyrimidine ring with NADPH is similar in the vertebrate and bacterial enzymes (difference of 1.3 kcal mol^{-1}). The electrostatics are accentuated here by the use of a dielectric of one and, even with this upper bound, make little difference. The favorable interactions arise predominantly from the spatial relationship between the trimethoxyphenyl ring of trimethoprim and NADPH. The trimethoxyphenyl ring occupies a different cleft in the chicken liver enzyme so that, in the *E. coli* system, this ring is within 4 Å of the nicotinamide of NADPH (the minimum atom–atom distance between the two groups is 3.2 Å) and its associated ribose (minimum distance of 2.5 Å), while the corresponding minimum distance is 3.5 Å from the nicotinamide and 6.0 Å from the ribose in the chicken liver ternary complex. As seen from Table VI, the van der Waals interactions between these groups of the NADPH and the trimethoprim phenyl ring are 2.2 kcal mol^{-1} more favorable in the *E. coli* complex. Coulombic interactions between the entire NADPH molecule and the trimethoxyphenyl ring are 3.1 kcal mol^{-1} more favorable in the *E. coli* ternary complex. These results reflect the proximity of the two ligands in the bacterial enzyme as seen in Fig. 5 (compare with Fig. 6 of the chicken liver complex). Along with the consideration of strain energy and protein–trimethoprim interactions discussed above, this supports the suggestion that it is the difference in trimethoprim–NADPH interactions that underlies the cooperativity in the *E. coli* complex.

CONCLUSIONS

We have carried out simulations of four dihydrofolate reductase complexes with several hundred waters using a force field that includes all cross terms and all hydrogen atoms. Thus, we have avoided the use of assumptions such as the united atom approximation, a restricted diagonal force field, or a cutoff value so that we can begin to assess some of these approximations. The internal regions of the protein of the minimized structures, such as the active site, fit the observed structures well. Large deviations are seen on the surface of the protein, which is less well-defined in the observed structures. This is expected as, in addition to the uncertainties in this region in the experimental structures, the crystal environment has not been included in the simulations and therefore intermolecular, lattice interactions with neighboring molecules in the lattice are absent.

Given the good fit of the internal region of the protein, we have then examined the basis for selectivity of trimethoprim in the *E. coli* and chicken liver enzymes. It was pointed out that uncertainties inherent in protein crystallographic coordinates lead to artifactual strain

energies in bond and valence angles, as well as large van der Waals interactions. Thus, energetic analysis was carried out on the fully minimized structures.

We have examined the intramolecular strain energy of trimethoprim and the effect of the binding of the trimethoxyphenyl ring of trimethoprim to different binding clefts in the *E. coli* and chicken liver DHFR's. Although the energetic analysis of the intramolecular strain energy of trimethoprim indicates that trimethoprim is more strained in the chicken liver binary complex than in the binary *E. coli* complex by 2.5 kcal mol^{-1}, this interaction is compensated for by the more favorable intermolecular interactions of the trimethoxyphenyl group of trimethoprim in the chicken liver binary complex (2.9 kcal mol^{-1} more favorable than in the binary *E. coli* enzyme). Thus, it appears that neither the intramolecular strain energy nor the intermolecular interactions of the trimethoxyphenyl group is a major factor for the enhanced binding of trimethoprim in *E. coli* DHFR.

Table VI. Non-Bonded Interactions of Trimethoprim with NADPH[a]

		E. coli Ternary			Chicken Liver Ternary		
NADPH	Energy	PRMD[b]	CH_2	Phenyl[c]	PRMD[b]	CH_2	Phenyl[c]
	VdW	−3.7	−0.6	−3.7	−3.6	−0.9	−1.9
Nicotinamide	Coul	−14.6	−1.7	−1.3	−14.0	−1.9	−0.3
	Total	−18.3	−2.3	−5.0	−17.6	−2.7	−2.2
Nicotinamide	VdW	−0.1	0.0	−0.7	−0.1	−0.1	−0.2
Ribose	Coul	5.7	0.6	0.2	5.7	0.7	0.1
	Total	5.6	0.5	−0.4	5.7	0.6	−0.1
Pyrophosphate	VdW	0.0	0.0	0.0	0.0	0.0	0.0
Linkage	Coul	−48.1	−4.6	−2.5	−48.2	−4.4	−1.0
	Total	−48.2	−4.6	−2.5	−48.2	−4.4	−1.1
Adenine	VdW	0.0	0.0	0.0	0.0	0.0	0.0
Ribose	Coul	−25.4	−2.1	−0.7	−24.9	−1.9	0.0
	Total	−25.4	−2.1	−0.7	−24.9	−1.9	0.0
	VdW	0.0	0.0	0.0	0.0	0.0	0.0
Adenine	Coul	−5.4	−0.5	−0.2	−5.4	−0.4	−0.1
	Total	−5.4	−0.5	−0.2	−5.4	−0.4	−0.1
	VdW	−3.8	−0.6	−4.4	−3.7	−0.9	−2.2
Total	Coul	−87.9	−8.3	−4.4	−86.7	−8.0	−1.3
	Total[d]	−91.7	−9.0	−8.8	−90.4	−8.9	−3.5

a. Energies in kcal mol^{-1}.
b. PRMD = 2,4-diaminopyrimidine.
c. Phenyl = 3,4,5-trimethoxyphenyl.
d. The total interaction of trimethoprim with NADPH in the *E. coli* ternary complex is −109.4 kcal mol^{-1}. The total energy of interaction of trimethoprim with NADPH in the chicken liver ternary complex is −102.8 kcal mol^{-1}.

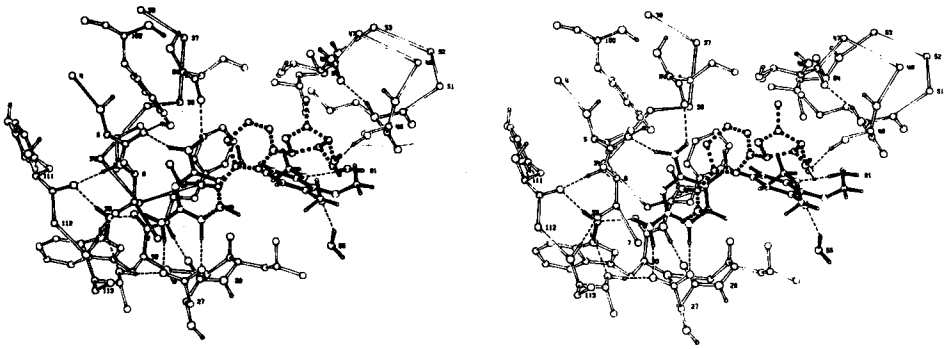

Fig. 5. Stereo plot of the active site of the minimized *E. coli* ternary complex with trimethoprim and waters 33, 55, and 91 indicated by solid bonds, NADPH (the nicotinamide group and its associated ribose only) by heavy dashed lines, protein residues by open bonds, and hydrogen bonds by dashed lines. The orientation is the same as for Fig. 2, conformation A of trimethoprim and close to the orientation of the schematics of Fig. 3.

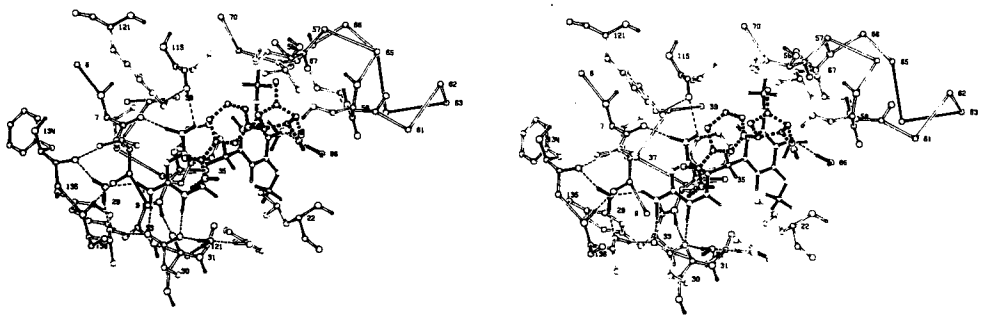

Fig. 6. Stereo plot of the active site of the minimized chicken liver ternary complex with trimethoprim and waters 29, 86, and 121 indicated by solid bonds, NADPH (the nicotinamide group and its associated ribose only) by heavy dashed lines, protein residues by open bonds, and hydrogen bonds by dashed lines. The orientation is the same as for Fig. 2, conformation B of trimethoprim and close to the orientation of the schematics of Fig. 3.

We have also examined the interaction energy between N4 of the pyrimidine ring of trimethoprim and the backbone carbonyl group of Val^{115} in chicken liver, implicated as a major factor in the poorer binding of trimethoprim in this enzyme compared with the *E. coli* enzyme. This interaction is calculated to be about 2 kcal mol^{-1} more favorable for an N–O distance of 2.9 Å, the observed distance in the bacterial enzyme, than for the N–O distance of 4.1 Å, the distance observed in the chicken liver enzyme. Thus, this may be an important factor in the difference of binding although the difference is not sufficient to explain the entire intrinsic enhanced binding to the *E. coli* enzyme of 5000. However, compensating effects were shown to introduce difficulties in assessing the cause of differences in binding energy to proteins from different species in terms of differences in single residue interactions. Such compensating effects could make interpretations based on experimental observation of different structures extremely perilous.

We have also investigated the source of the cooperativity exhibited in the *E. coli* enzyme. The cooperativity of NADPH was found to be due to more favorable energetics between the cofactor and the trimethoxyphenyl ring of trimethoprim in the *E. coli* complex because of better van der Waals interactions between these groups in that enzyme. Although it has been suggested that the binding of NADPH may lead to more favorable interactions of trimethoprim with the *E. coli* enzyme, our calculations indicate that this is not the case. Instead, as might be expected, NADPH binding decreases this interaction.

Acknowledgements. This work was supported by NIH grant GM30564. We would also like to thank Control Data Corpora-Corporation for awarding a PACER postdoctoral fellowship to David Osguthorpe.

REFERENCES

1. R. L. Blakley, *The Biochemistry of Folic Acid and Related Pteridines*, North-Holland, Amsterdam, 1969.
2. M. Friedkin, *Adv. Enzymol.*, **38**, 235 (1973).
3. J. E. Gready, *Adv. Pharmacol. Chemother.*, **17**, 37 (1980).
4. J. Burchall and G. H. Hitchings, *Mol. Pharmacol.*, **1**, 126 (1965).
5. B. R. Baker in A. Burger, ed., *Medicinal Chemistry*. Wiley–Interscience, New York, 1970, pp. 196–228.
6. D. A. Matthews, J. T. Bolin, J. M. Burridge, D. J. Filman, K. W. Volz and J. Kraut, *J. Biol. Chem.*, **260**, 392 (1985).
7. S. R. Stone and J. F. Morrison, *Biochim. Biophys. Acta*, **869**, 275 (1986).
8. P. Dauber, D. J. Osguthorpe and A. T. Hagler, *Biochem. Soc. Trans.*, **10**, 312 (1982).
9. D. A. Matthews, J. T. Bolin, J. M. Burridge, D. J. Filman, K. W. Volz, B. T. Kaufman, C. R. Beddell, J. N. Champness, D. K. Stammers and J. Kraut, *J. Biol. Chem.*, **260**, 381 (1985).
10. D. A. Matthews, R. Alden, J. T. Bolin, S. T. Freer, R. Hamlin, N. Xuong, J. Kraut, M. Poe, M. Williams and K. Hoogstein, *Science*, **197**, 452 (1977).
11. D. A. Matthews, R. A. Alden, J. T. Bolin, D. J. Filman, S. T. Freer, R. Hamlin, W. G. J. Hol, R. L. Kisliuk, E. J. Pastore, L. T. Plante, N. Xuong and J. Kraut, *J. Biol. Chem.*, **253**, 6946 (1978).
12. D. A. Matthews, R. A. Alden, S. T. Freer, N. Xuong and J. Kraut, *J. Biol. Chem.*, **254**, 4144 (1979).
13. K. W. Volz, D. A. Matthews, R. A. Alden, S. T. Freer, C. Hansch, B. T. Kaufman and J. Kraut, *J. Biol. Chem.*, **257**, 2528 (1982).
14. J. T. Bolin, D. J. Filman, D. A. Matthews, R. C. Hamlin and J. Kraut, *J. Biol. Chem.*, **257**, 13650 (1982).
15. D. J. Filman, J. T. Bolin, D. A. Matthews and J. Kraut, *J. Biol. Chem.*, **257**, 13653 (1982).
16. M. Karplus and J. A. McCammon, *CRC Crit. Rev. Biochem.*, **9**, 293 (1981).
17. A. T. Hagler, Theoretical Simulation of Conformation, Energetics, and Dynamics of Peptides, in S. Udenfriend, J. Meienhofer, V. J. Hruby eds., *The Peptides*, **7**, 1985, pp. 213–299.
18. G. Wipff, A. Dearing, P. K. Weiner, J. M. Blaney and P. A. Kollman, *J. Am. Chem. Soc.*, **105**, 997 (1983).
19. J. M. Blaney, P. K. Weiner, A. Dearing, P. A. Kollman, E. C. Jorgensen, S. J. Oatley, J. M. Burridge and C. C. F. Blake, *J. Am. Chem. Soc.*, **104**, 6424 (1982).
20. M. Levitt, *J. Mol. Biol.*, **168**, 595 (1983).
21. W. F. van Gunsteren, H. J. C. Berendsen, J. Hermans, W. G. J. Hol and J. P. M. Postma, *Proc. Natl. Acad. Sci. USA*, **80**, 4315 (1983).
22. M. K. Gilson, A. Rashin, R. Fine and B. Honig, *J. Mol. Biol.*, **183**, 503 (1985).
23. J. G. Kirkwood, *J. Chem. Phys.*, **2**, 351 (1934).
24. J. G. Kirkwood and F. H. Westheimer, *J. Chem. Phys.*, **6**, 506 (1938).
25. G. N. Ramachandran and R. Srinivasan, *Ind. J. Biochem.*, **7**, 95 (1970).
26. A. T. Hagler in J. Hermans, ed., *Molecular Dynamics and Protein Structure*, Polycrystal Book Service, Western Springs, Illinois, 1984, pp. 133–138.
27. A. T. Hagler, E. Huler and S. Lifson, *J. Am. Chem. Soc.*, **96**, 5319 (1974).

28. A. T. Hagler and S. Lifson, *J. Am. Chem. Soc.*, **96**, 5327 (1974).
29. S. Lifson, A. T. Hagler and P. Dauber, *J. Am. Chem. Soc.*, **101**, 5111 (1979).
30. A. T. Hagler, S. Lifson and P. Dauber, *J. Am. Chem. Soc.*, **101**, 5122 (1979).
31. A. T. Hagler, P. Dauber and S. Lifson, *J. Am. Chem. Soc.*, **101**, 5131 (1979).
32. A. T. Hagler, P. S. Stern, R. Sharon, J. M. Becker and F. Naider, *J. Am. Chem. Soc.*, **101**, 6842 (1979).
33. T. L. Hill, *An Introduction to Statistical Thermodynamics*, Addison-Wesley, Reading, Mass., 1960.
34. A. T. Hagler, E. Huler and S. Lifson, The Amide Hydrogen Bond in Energy Functions for Peptides and Proteins, in E. R. Blout, F. A. Bovey, M. Goodman and N. Lotan, eds., *Peptides, Polypeptides and Proteins*, Wiley, N.Y., 1974, pp. 35–48.
35. T. F. Koetzle and G. J. B. Williams, *J. Am. Chem. Soc.*, **98**, 2074 (1976).
36. W. E. Oberhansli, *Helv. Chim. Acta*, **53**, 1787 (1970).
37. A. Makriyannis and S. Fesik, *J. Am. Chem. Soc.*, **104**, 6462 (1982).
38. D. P. Baccanari, S. Daluge and R. W. King, *Biochemistry*, **21**, 5068 (1982).
39. B. Birdsall, G. C. K. Roberts, J. Feeney, J. G. Dann and A. S. V. Burgen, *Biochemistry*, **22**, 5597 (1983).
40. W. P. Jencks, *Adv. Enzymol.* **43**, 219 (1975).
41. A. T. Hagler, P. S. Stern, S. Lifson and S. Ariel, *J. Am. Chem. Soc.*, **101**, 813 (1979).
42. S. Subramanian and B. T. Kaufman, *Proc. Natl. Acad. Sci. USA*, **75**, 3201 (1978).
43. M. Poe, K. Hoogsteen and D. A. Matthews, *J. Biol. Chem.*, **254**, 8143 (1979).